Journal of Materials Chemistry C

Accepted Manuscript

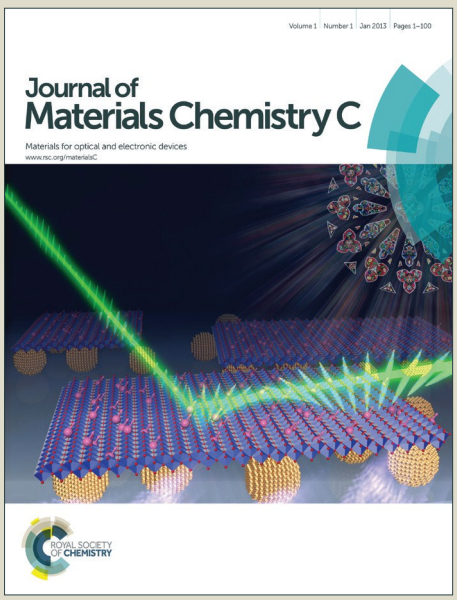

ROYAL SOCIETY OF CHEMISTRY

www.rsc.org/materialsC

Cite this: DOI: 10.1039/c0xx00000x

www.rsc.org/xxxxxx

ARTICLE TYPE

EuS-CdS and EuS-ZnS Heterostructured Nanocrystals Constructed from Co-thermal Decomposition of Molecular Precursors in Solution Phase

Xueyun Gong,[a,b,c] Zhengqing Liu,[a] Dong Yan,[a] Hongyang Zhao,[a] Na Li,[a] Xinyu Zhang,[a] and Yaping Du*[a,c]

Received (in XXX, XXX) Xth XXXXXXXXX 20XX, Accepted Xth XXXXXXXXX 20XX
DOI: 10.1039/b000000x

The EuS-CdS and EuS-ZnS heterostructured nanocrystals have been synthesized from a facile co-thermal decomposition method. The as-obtained nanoheterostructures hold the unique optical-magnetic dual modal properties.

In recent years, heterostructured nanocrystals (NCs) have inspired great research interest owing to their integrated multifunctionality of different components. Such multifunctionality endows heterostructured NCs great potential in board scientific and technological research areas such as optics, electronics, catalysis, sensors, biomedicine, energy conversion and storage, and so on.[1–17] The efficient synthesis of diverse heterostructured NCs with desired chemical composition, uniform size and morphology *via* facile and economical chemical synthesis strategies, and the exploration of multifunctional material properties and various potential applications, has become the most stimulating subjects faced by many material chemists.[1–21]

Lanthanide compound NCs have received tremendous attention due to their specific properties arising from the 4*f* electron configuration of the lanthanides, particularly, lanthanide chalcogenides have long been acknowledged for their promising applications in various fields including luminescent materials and permanent magnets, i.e. europium monochalcogenides, EuX (X = O, S, Se, Te), with a rock-salt structure, have been investigated extensively and well known to have a wide range of applications such as ferromagnetic semiconductors, optomagnetic, magnetoresistance, and luminescent materials.[22-32]

As an important category of nanoheterostructures, lanthanide chalcogenides based heterostructured NCs and their nanocomposites have received growing attention for investigating their multifunctional properties and potential applications. Thus, great efforts have been devoted to fabricating different lanthanide chalcogenides nanoheterostructures and their alternatives (such as doping and/or composites), and a diversity of material composition has also been achieved and favored their applications in many fields.[33–36]

However, up to present, very little research focused on the construction and synergetic properties of lanthanide chalcogenides and semiconductor combined nanoheterostructures. For example, Scholes et al. synthesized EuS-CdS nanoheterostructures with a broken band alignment *via* a two-step synthetic approach, in which, cadmium oxide firstly reacted with selenium powder to form cadmium selenide followed by injecting the precursor of $Eu(ddtc)_3(bipy)$ (ddtc = diethyldithiocarbamate, bipy = bipyridyl). Through "anion displacement" to attain CdS stems and finally formed EuS-CdS nanoheterostructures.[37] Sasaki et al. prepared core-shell structured PbS@EuS NCs employing the similar way. Firstly, the PbS core material was obtained by reacting lead chloride and sulfur powder in oleylamine solvent. Subsequently, the EuS shell was deposited from the thermal decomposition of $(PPh_4)[Eu(ddtc)_4]$ (PPh_4 = tetraphenyl phosphine) at a high temperature of 300 °C.[38]

Based on our previous work in terms of synthesis and properties of high quality lanthanide-containing and metal sulfides NCs,[39–43] in this communication, *for the first time*, we reported a general and robust way to synthesize EuS-CdS and EuS-ZnS heterostructured NCs by co-thermal decomposition of molecular precursors of $Cd(ddtc)_2$ or $Zn(ddtc)_2$ and $Eu(ddtc)_3(Phen)$ (Phen = phenanthroline), which is much more convenient and advanced than the commonly used seeded growth or catalyst-assisted growth method. In addition, the as-obtained heterostructured NCs possessed interesting optical-magnetic bimodal properties (Scheme 1).

Scheme 1 Illustration of co-thermal decomposition synthesis of EuS-CdS heterostructured nanocrystals.

The crystal phase of as-synthesized EuS-CdS product was examined with powder X-ray diffraction analysis (XRD, Fig. 1a). The diffraction peaks for EuS-CdS product can be readily indexed to hexagonal phase of CdS with lattice constant of $a = b = 4.141$ Å, $c = 6.720$ Å (wutzite type, space group: *P63mc*,

JCPDS: 41–1049) and cubic phase of EuS with lattice constant of $a = b = c = 5.967$ Å (rock salt, space group: *Fm-3m*, JCPDS: 26–1419). No diffraction peaks from any other chemical species such as lanthanide oxides and oxysulfide (i.e. EuO and Eu_2O_2S) were detectable. The broadening of the diffraction peaks is an indication of the sample's nano-crystalline nature. In addition, the energy-dispersive X-ray analysis (EDAX), which was detected in three different areas of the scanning electron microscopy (SEM) substrate) clearly illustrated in Fig. S1† and Table S1† indicated the existence of Cd, Eu and S elements in the as-formed EuS-CdS samples. Fig. 1b depicted a typical transmission electron microscopy (TEM) image of EuS-CdS heterostructured NCs prepared with an $Cd(ddtc)_2/Eu(ddtc)_3(Phen)$ molar ratio of 3:1 in the presence of a surfactant mixture including oleic acid and oleylamine. The heterostructured NCs were of uniform shape with obvious difference in the mass-thickness contrast between the head and the stem, demonstrating the various chemical compositions of the as-prepared NCs. The stem had the size of ~11 nm in length and ~9 nm in width, and the head had a thickness of ~2 nm. Moreover, there were two configurations existed in our nanoheterostructures, one was the head grew on one side of stem, the other was the head grew on both two sides of stem (Fig. 1b). It can be estimated approximately 70% of the obtained nanocrystals are the heterostructures (statistic from at least 50 particles). Fig. 1c showed the high-angle annular dark field-scanning TEM (HAADF-STEM) image of EuS-CdS heterostructured NCs. It was clearly observed that the EuS and CdS component in individual nanocrystal, featured comparatively high and low intensity for each phase, and the lighter and darker areas represented the EuS and CdS parts, respectively, since the EuS phase was a stronger scatterer than CdS at high angles in accordance with the basic rule $I \propto Z^2$ (I : intensity, Z : atomic number) for HAADF-STEM images. The inset of Fig. 1c showed the photograph of colloidal EuS-CdS heterostructured NCs dispersed in cyclohexane, and there was no evident sedimentation even after having been stored for more than 1 month at room temperature.

A high-resolution TEM (HRTEM) image of a typical EuS-CdS heterostructured nanocrystal was shown in Fig. 1d. The as-obtained nanoheterostructures were highly crystalline with the similar nanorod-like head and stem, and had a partially coherent interface between single-crystalline head and stem. The lattice spacings of head was measured to be ~0.298 nm, identical to the distances of the (200) plane of bulk EuS. The fringes with a lattice spacing of ~0.336 nm was observed for CdS stem, corresponding to the (002) plane of bulk CdS. All in all, based on the analysis of the corresponding heterostructures' crystal lattices, the head is composed of EuS and the stem is CdS, and the conjunction interface consists of the (002) crystal plane of the CdS stem and the (200) crystal plane of the EuS head. Meanwhile, the size and morphology distribution histogram was shown in Fig. S2a†-S2d†.

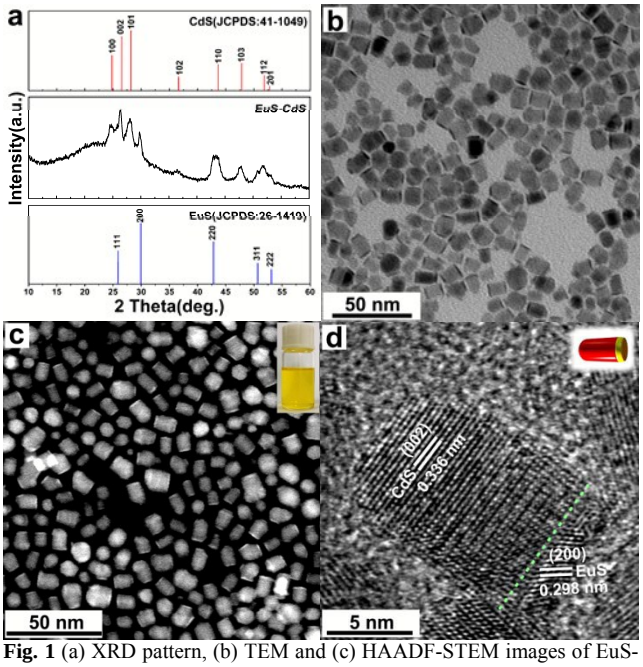

Fig. 1 (a) XRD pattern, (b) TEM and (c) HAADF-STEM images of EuS-CdS heterostructured NCs; The inset photograph of colloid EuS-CdS heterostructured NCs dispersed in cyclohexane, which have been placed in an ambient environment for more than 1 month; d) HRTEM image of a representative EuS-CdS heterostructured nanocrystal, the inset shows the schematic diagram of a nanoheterostructure.

The modeling structure of EuS-CdS nanoheterostructure was shown in Fig. 2. The unit cell of the hexagonal CdS and cubic EuS was illustrated in Fig. 2a and Fig. 2b, respectively. Fig. 2c demonstrated the (002) crystal plane of CdS crystal viewed from the <001> direction, according to the lattice parameters of hexagonal CdS ($a = b = 4.141$ Å, $c = 6.720$ Å), the calculated distance of the adjacent cadmium atom was ~0.414 nm; Fig. 2d showed the (111) crystal plane of EuS crystal viewed from the <1–10> direction, according to the lattice parameters of the cubic EuS ($a = b = c = 5.967$ Å), the calculated distance of the adjacent europium atom was ~0.422 nm($\sqrt{2}/2\times$a), close to the distance of the adjacent cadmium atom (0.414 nm). Additionally, since the ion radius of Cd^{2+} is 0.097 nm, which is very close to the radius of Eu^{2+} (0.109 nm), the Cd^{2+} could be easily replaced by Eu^{2+} to form EuS-CdS heterostructured NCs. Fig. 2e exhibited the modeling structure of a typical EuS-CdS nanoheterostructure, the (002) crystal plane of CdS and the (200) crystal plane of EuS was marked out, respectively, which was perfect matched well with the as-observed single HRTEM of EuS-CdS heterostructured nanocrystal. In addition, the calculated angle of (002) crystal plane of CdS and (200) crystal plane of the EuS in the modeling was calculated to be ~54.74º, which was also matched well with the measured angle (~54º) from the as-observed single HRTEM of EuS-CdS nanocrystal.

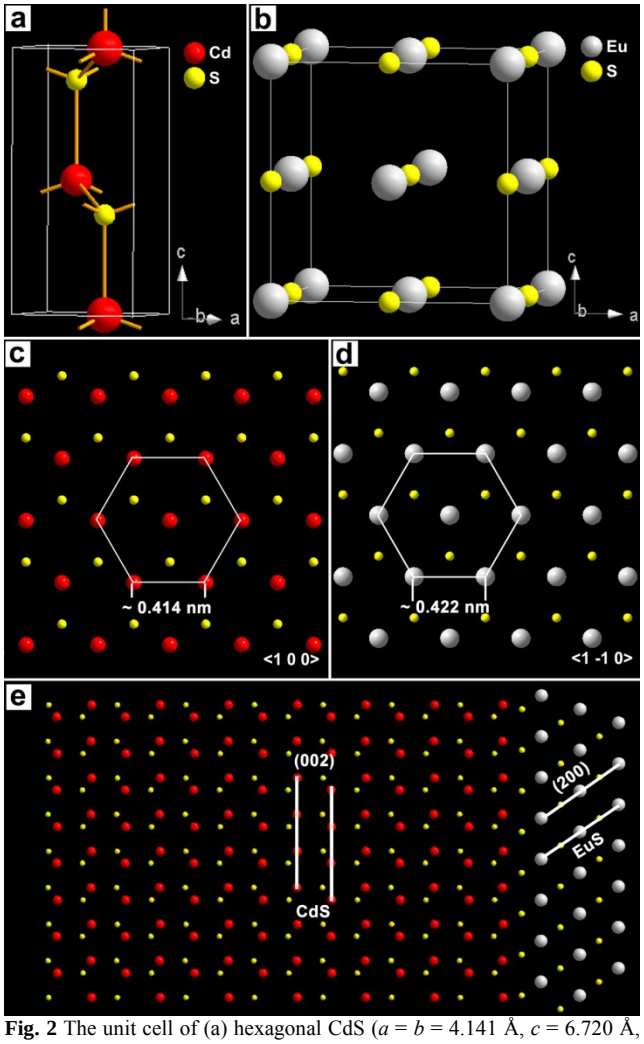

Fig. 2 The unit cell of (a) hexagonal CdS ($a = b = 4.141$ Å, $c = 6.720$ Å, space group: *P63mc*, JCPDS: 41–1049) and (b) cubic EuS ($a = b = c = 5.967$ Å, space group:*Fm-3m*, JCPDS: 26–1419); (c) (002) crystal plane of the CdS viewed from the <001> direction and (d) (111) crystal plane of the EuS viewed from the <1–10> direction; (e) The modeling structure of a representative EuS-CdS heterostructured nanocrystal.

X-ray photoelectron spectroscopy (XPS) technique was employed to analyze surface chemical composition of as-obtained EuS-CdS heterostructured NCs. Panels a-c of Fig. 3 showed the XPS signals taken from the Cd 3d, S 2p, and Eu 4d regions of the EuS-CdS heterostructured NCs. As seen from Fig. 3a, the double peaks at 411.6 and 404.9 eV were assigned to the Cd $3d_{3/2}$ and Cd $3d_{5/2}$ of Cd^{2+} ions, respectively. The peaks shown in Fig. 3b located at 162.6 and 161.4 eV could be assigned to the binding energies of S $2p_{1/2}$ and S $2p_{3/2}$, respectively, which were separated by a spin-orbit splitting of 1.2 eV. The peaks at 141.1 and 136.1 eV in Fig. 3c were assigned to the Eu $4d_{3/2}$ and Eu $4d_{5/2}$ of Eu^{3+} ions, while the peaks at 128.1 eV was assigned to the Eu 4d of Eu^{2+} ions, suggesting that the Eu^{2+} ions on the surface was partly oxidized to Eu^{3+} ions while exposing in air, which is consistent with the reported results.[44] The Fourier transform infrared spectroscopy (FTIR) spectra of the as-synthesized EuS-CdS heterostructured NCs was shown in Fig. S3†. The peaks located at 2950 and 2800 cm^{-1} reveal the C–H stretching, suggesting the existence of free oleylamine. The broad peaks at 1465 cm^{-1} and 1500 cm^{-1} were assigned to carboxylate (COO-) stretching[45] and N–H stretching mode, respectively. In addition, the peak at 883 cm^{-1} was assigned to the C–N stretching mode of alkylamine. Based on the FTIR analysis, it can be deduced that the synthesized EuS-CdS heterostructured NCs are capped by oleic acid and oleylamine surfactants.

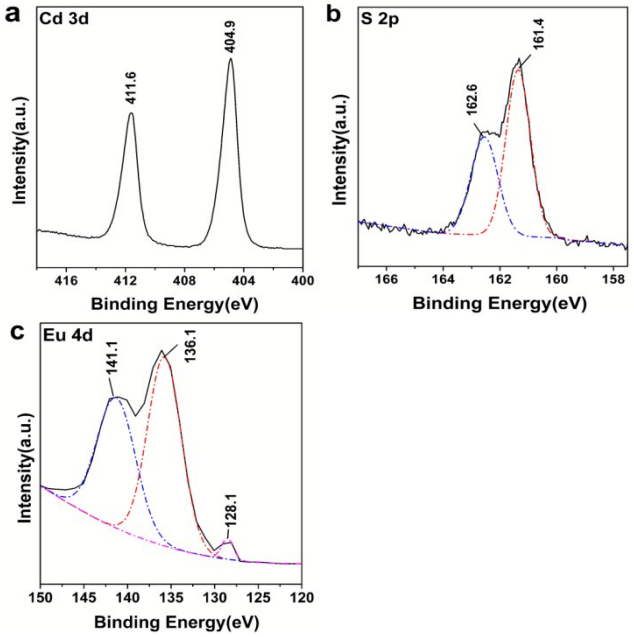

Fig. 3 XPS spectra of a) Cd 3d, b) S 2p, c) Eu 4d signals recorded for EuS-CdS heterostructured NCs.

Note that we have carried out a series of experiments to optimize the conditions for synthesis of EuS-CdS heterostructured NCs with high quality. In our synthesis, the mole ratios of two molecular precursors, the compositions of surfactants, as well as the reaction temperature and time were found to play crucial roles in the formation of high quality EuS-CdS heterostructured NCs. For example, under the same reaction condition, i.e. the solvents composition of oleic acid (3 mmol), oleylamine (18 mmol) and l-octadecene (20 mmol), the reaction temperature was 280 °C, and $Cd(ddtc)_2$ was fixed as 0.5 mmol while varying the mole ratio of $Cd(ddtc)_2/Eu(ddtc)_3(Phen)$ to 9:1, 7:1, 5:1, 4:1, 3:1 and 1:1. When the mole ratio was 9:1 and 7:1, hardly EuS components were found in the final products (Fig. S4a† and S4b†). The EuS-CdS heterostructured NCs were gradually appeared along with increasing the amount of $Eu(ddtc)_3(Phen)$ (Fig. S4c† and S4d†). However, as further accumulating the $Eu(ddtc)_3(Phen)$ concentration, it was found that EuS species separated from the CdS components (Fig. S4e†). To conclude, the EuS-CdS heterostructured NCs with high yields were only harvested at an optimized $Cd(ddtc)_2/Eu(ddtc)_3(Phen)$ ratio of 3:1 (Fig. S4f†). Besides the mole ratio of precursors, it was found that the composition of surfactants was essential for the preparation of high quality EuS-CdS heterostructured NCs. For instance, at a fixed experimental condition, i.e. the mole ratio of $Cd(ddtc)_2$ and $Eu(ddtc)_3(Phen)$ was 3:1 (0.3 mmol : 0.1 mmol) and the reaction temperature was 280 °C, when the mole ratio of surfactants of oleic acid and oleylamine was increased to 3:1 (15 mmol : 5 mmol), only severely aggregated products with poor dispersibility were harvested (Fig. S4g†), while the mole ratio of

oleic acid and oleylamine was decreased to 1:9 (2 mmol : 18 mmol) resulted in some unshapely EuS-CdS heterostructured NCs with rather low yields (Fig. S4h†). On the other hand, we also found that both the reaction temperature and time remarkably affected the quality of the products. For example, at a fixed experimental condition, i.e. 0.3 mmol of $Cd(ddtc)_2$ and 0.1 mmol of $Eu(ddtc)_3(Phen)$, oleic acid (3 mmol), oleylamine (18 mmol) and l-octadecene (20 mmol), when the reaction temperature was decreased below 270 °C, the as-obtained products presented two different separated phases (Fig. S4i†–S4k†). This experimental phenomenon could be explained from thermogravimetric analysis of the precursors (Fig. S5a†–S5c†). As indicated from the thermogravimetric analysis, three molecule precursors, namely, $Cd(ddtc)_2$, $Zn(ddtc)_2$, $Eu(ddtc)_3(Phen)$, their decomposing temperature for targeted compound is about 310 °C, 330 °C and 300 °C, respectively. Therefore, when the reaction temperature below 270 °C, there were deficient energy for the formation of EuS-CdS heterostructured NCs, while, further elevating the temperature to 300 °C yielded the aggregated heterostructured NCs with broad size distribution (Fig. S6a†). Moreover, at the fixed reaction temperature of 280 °C, prolonging the reaction time to 1 h after the injection of $Eu(ddtc)_3(Phen)$, the as-formed EuS-CdS heterostructured NCs with broad size and shape distribution together with segregated EuS and CdS nanoparticles were obtained (Fig. S6b†).

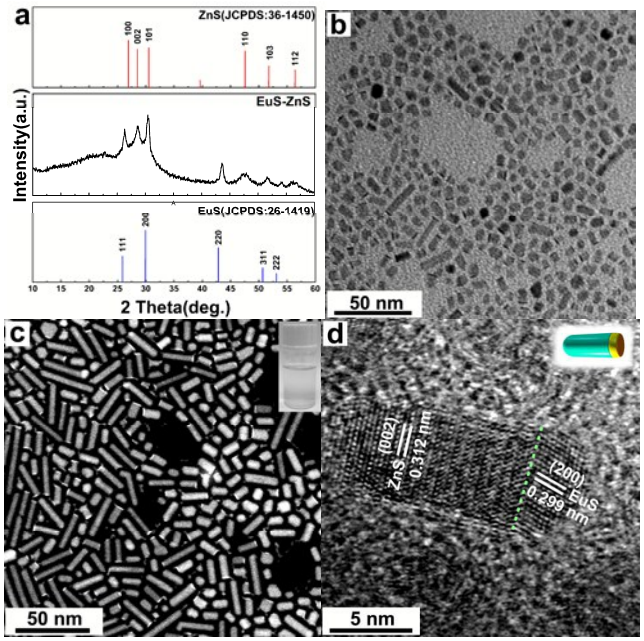

Fig. 4 (a) XRD pattern, (b) TEM and (c) HAADF-STEM images of EuS-ZnS heterostructured NCs, the inset photograph of colloid EuS-ZnS heterostructured NCs dispersed in cyclohexane, which have been placed in an ambient environment for more than 1 month; (d) HRTEM image of a representative EuS-ZnS heterostructured nanocrystal, the inset shows the schematic diagram of a nanoheterostructure.

Our current method is general and robust as it can be readily extended to synthesize other EuS based nanoheterostructures. For example, with employing the same synthesis strategy, i.e. the molar ratio of $Zn(ddtc)_2/Eu(ddtc)_3(Phen)$ was 3:1 (0.3 mmol : 0.1 mmol), solvents composition of 3 mmol of oleic acid, 18 mmol of oleylamine, and 20 mmol of l-octadecene, the reaction temperature was 280 °C, and reaction time lasts for 5 min, the EuS-ZnS nanoheterostructures were harvested, as evidenced by XRD and TEM characterizations (Fig. 4a-b). The diffraction peaks from Fig. 4a for EuS-ZnS heterostructures can be indexed to hexagonal phase ZnS with lattice constant of a = 3. 821 Å, b = 3. 821 Å, c = 6.257 Å (space group: *P63mc*, JCPDS: 36–1450) and cubic phase of EuS with lattice constant of $a = b = c$ = 5.967 Å (space group: *Fm-3m*, JCPDS: 26–1419). In addition, the EDAX results (Fig. S7a† and Table S2†) also confirmed the existence of Zn, Eu and S elements in our EuS-ZnS nanoheterostructures.

As shown in TEM and HAADF-STEM images (Fig. 4b-c), the morphology of EuS-ZnS heterostructured NCs resembled that of the EuS-CdS, but with the stem size varied from ~5 nm to ~30 nm in length and ~5 nm in width, and the head thickness of ~2 nm. Similarly, a HRTEM image of a typical EuS-ZnS was shown in Fig. 4d. The fringes with a lattice spacing of 0.312 nm and 0.299 nm were clearly observed, corresponding to the (002) crystal planes for ZnS and (200) for EuS, respectively. On the other hand, similar to the EuS-CdS, both the FTIR (Fig. S7b†) and XPS (Fig. S8†) characterizations were adopted to analyze the obtained EuS-ZnS heterostructured NCs.

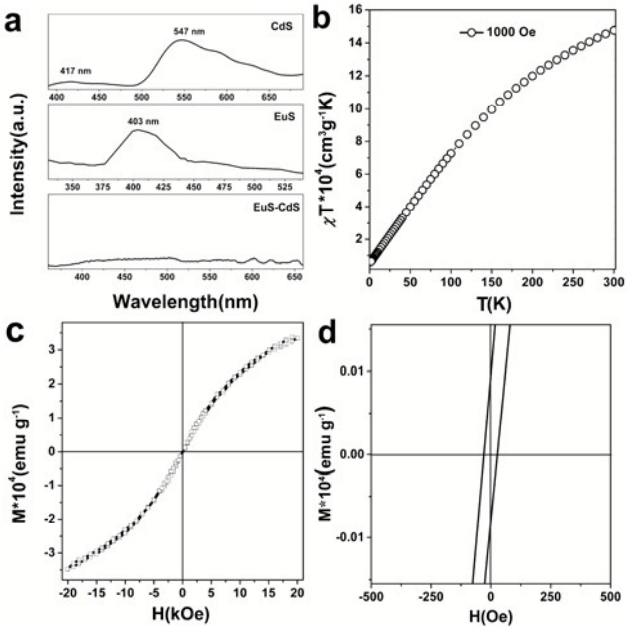

Fig. 5 (a) PL spectra of CdS, EuS and EuS-CdS heterostructured NCs dispersed in cyclohexane solvent; (b) Temperature dependence of the inverse magnetic susceptibility χT and (c, d) the hysteresis loop of EuS-CdS heterostructured NCs.

Obtaining highly quality EuS-CdS heterostructured NCs enabled further investigation of their synergistic optical and magnetic properties. Fig. 5a demonstrated the photoluminescence (PL) spectra of CdS, EuS (under the similar reaction condition of synthesizing EuS-CdS rather than by using $Cd(ddtc)_2$ and $Eu(ddtc)_3(Phen)$ as sole decomposing precursor) and EuS-CdS heterostructured NCs dispersed in cyclohexane. The PL spectrum of CdS NCs at an excitation wavelength of 360 nm presented a broad emission at ~547 nm resulted from the sulfur vacancies in CdS NCs and a emission peak at ~417 nm due to direct electron-

hole recombination.[46] The PL spectrum of EuS NCs at an excitation wavelength of 290 nm exhibited a emission at ~403 nm due to the 4f–5d transition of Eu^{2+}.[47,48] Notably, we found that the photoluminescence intensity of EuS-CdS heterostructured NCs was too weak even to observe, and this phenomenon was very similar to that of results observed by Scholes et al.,[37] where, they explained that the conduction band of CdS could be populated by EuS valence states through wave function leakage, thus leading to band filling or quasi band filling and the as-resulting photoluminescence quenching. The energy band structure scheme of EuS-CdS heterostructured NCs was shown in Fig. S9†.

Magnetic properties of our EuS-CdS heterostructured NCs were investigated using a superconducting quantum interference device (SQUID) magnetometer. The temperature dependence of the magnetization was shown in Fig. 5b, which was related to the reverse magnetic susceptibility versus temperature from 300 to 2 K. The anomalous magnetic phenomenon of slight increases of χT above 10 K was observed, similar to the ferrimagnetism at a relatively high temperature, which may originate from the contribution of Eu^{3+} ions on the surface.[49] Fig. 5c illustrated the magnetization behaviors of EuS-CdS heterostructured NCs at 2 K from an applied magnetic field from -20 to 20 kOe. Moreover, the hysteresis loop shown in Fig. 5d indicated that the EuS-CdS heterostructured NCs had a coercive field of almost 30 Oe at 2 K.

Conclusions

In summary, we have firstly demonstrated a facile and robust way to synthesize EuS-CdS and EuS-ZnS heterostructured NCs through co-thermal decomposition of molecular precursors of $Eu(ddtc)_3(Phen)$ and $Cd(ddtc)_2/Zn(ddtc)_2$ in oleic acid, oleylamine and 1-octadecene. The as-obtained lanthanide chalcogenides based nanoheterostructures exhibited unique optical and magnetic dual modal properties, which may pave new avenue for potential applications for bio-imaging and MRI (magnetic resonance imaging) applications. We believe that our strategy could be broadly applicable for the facile production of other novel lanthanide compound based nanoheterostructures with great promise for various applications.

Notes and references

[a] *Frontier Institute of Science and Technology jointly with College of Science, State Key Laboratory for Mechanical Behavior of Materials, Xi'an 710049, China.*
E-mail: ypdu2013@mail.xjtu.edu.cn; ypdupku@gmail.com; Tel&Fax: 86-29-83395385
[b] *College of Physics and Chemistry, Henan Polytechnic University, Jiao'zuo, Henan Province, 454000, China.*
[c] *Key Laboratory of Synthetic and Natural Functional Molecule Chemistry of Ministry of Education, College of Chemistry & Materials Science, Northwest University, Xi'an, Shaanxi, 710069, China.*

Acknowledgements

We gratefully acknowledge the financial aid from the start-up founding from Xi'an Jiaotong University (XJTU) and the National Nature Science Foundation of China (NSFC, Grant No. 21371140 and No. 51205111). Prof. Yan-Zhen Zheng and Mr. Yue-Qiao Hu in XJTU are greatly acknowledged for their magnetic property characterization and analysis. We also appreciated Dr. Xing-Hua Li in Northwest University for his kind helps to obtain TEM images.

† Electronic Supplementary Information (ESI) available: The experimental details and other characterization are provided. See DOI: 10.1039/b000000x/

[1] J. T. Zhang, Y. Tang, K. Lee and M. Ouyang, *Science* 2010, **327**, 1634–1638.
[2] R. D. Robinson, B. Sadtler, D. O. Demchenko, C. K. Erdonmez, L. W. Wang and A. P. Alivisatos, *Science* 2007, **317**, 355–358.
[3] M. R. Buck, J. F. Bondi, R. E. Schaak, *Nat. Chem.* 2012, *4*, 37–44.
[4] S. E. Habas, H. Lee, V. Radmilovic, G. A. Somorjai and P. D. Yang, *Nat. Mater.* 2007, **6**, 692–697.
[5] H. Yu, M. Chen, P. M. Rice, S. X. Wang, R. L. White and S. H. Sun, *Nano Lett.* 2005, **5**, 379–382.
[6] N. J. Borys, M. J. Walter, J. Huang, D. V. Talapin and J. M. Lupton, *Science* 2010, **330**, 1371–1374.
[7] L. X. Yi, Y. Y. Liu, N. L. Yang, Z. Y. Tang, H. J. Zhao, G. H. Ma, Z. G. Su and D. Wang, *Energy Environ. Sci.* 2013, **6**, 835–840.
[8] D. S. Wang and Y. D. Li, *Adv. Mater.* 2011, **23**, 1044–1060.
[9] B. Xu, P. L. He, H. L. Liu, P. P. Wang, G. Zhou and X. Wang, *Angew. Chem. Int. Ed.* 2014, **53**, 2339–2343.
[10] R. Costi, A. E. Saunders and U. Banin, *Angew. Chem. Int. Ed.* 2010, **49**, 4878–4897.
[11] C. Wang, C. Xu, H. Zeng and S. H. Sun, *Adv. Mater.* 2009, **21**, 3045–3052.
[12] P. D. Cozzoli, T. Pellegrino and L. Manna, *Chem. Soc. Rev.* 2006, **35**, 1195–1208.
[13] J. Z. Chen, X. J. Wu, L. S. Yin, B. Li, X. Hong, Z. X. Fan, B. Chen, C. Xue and H. Zhang, *Angew. Chem. Int. Ed.* 2015, **54**, 1210–1214.
[14] X. Huang, Z. Y. Zeng, S. Y. Bao, M. F. Wang, X. Y. Qi, Z. X. Fan and H. Zhang, *Nat. Commun.* 2013, **4**, 1444.
[15] Z. Y. Zeng, C. L. Tan, X. Huang, S. Y. Bao and H. Zhang, *Energy Environ. Sci.* 2014, **7**, 797–803.
[16] W. J. Zhou, Z. Y. Yin, Y. P. Du, X Huang, Z. Y. Zeng, Z. X. Fan, H. Liu, J. Y. Wang and H. Zhang, *Small* 2013, **9**, 140–147.
[17] X. Hong, Z. Y. Yin, Z. X. Fan, Y. Y. Tay, J. Z. Chen, Y. P. Du, C. Xue, H. Y. Chen and H. Zhang, *Small* 2014, 10, 479–482.
[18] A. W. Tang, L. X. Yi, W. Han, F. Teng, Y. S. Wang, Y. B. Hou and M. Y. Gao, *Appl. Phys. Lett.* 2010, **97**, 033112.
[19] W. Han, L. X. Yi, N. Zhao, A. W. Tang, M. Y. Gao and Z. Y. Tang, *J. Am. Chem. Soc.* 2008, **130**, 13152–13161.
[20] L. X. Yi, A. W. Tang, M. Niu, W. Han, Y. B. Hou and M. Y. Gao, *CrystEngComm.* 2010, **12**, 4124–4130.
[21] T. Mokari, E. Rothenberg, I. Popov, R. Costi and U. Banin, *Science* 2004, **304**, 1787–1790.
[22] Y. Hasegawa, T. Adachi, A. Tanaka, M. Afzaal, P. O'Brien, T. Doi, Y. Hinatsu, K. Fujita, K. Tanaka and T. Kawai, *J. Am. Chem. Soc.* 2008, **130**, 5710–5715.
[23] M. D. Regulacio, S. Kar, E. Zuniga, G. B. Wang, N. R. Dollahon, G. T. Yee and S. L. Stoll, *Chem. Mater.* 2008, **20**, 3368–3376.
[24] Y. Hasegawa, M. Maeda, T. Nakanishi, Y. Doi, Y. Hinatsu, K. Fujita, K. Tanaka, H. Koizumi and K. Fushimi, *J. Am. Chem. Soc.* 2013, **135**, 2659–2666.
[25] A. Tanaka, H. Kamikubo, Y. Doi, Y. Hinatsu, M. Kataoka, T. Kawai and Y. Hasegawa, *Chem. Mater.* 2010, **22**, 1776–1781.
[26] P. Wachter, *Handbook on the Physics and Chemistry of Rare Earths, 2nd edn*; North-Holland Publishing Company: Amsterdam, 1979, pp. 189–241.
[27] A. Maguer and C. Godart, *Phys. Rep*. 1986, **141**, 51–176.
[28] K. Tanaka, K. Fujita, N. Soga, J. R. Qiu and K. Hirao, *J. Appl. Phys*. 1997, **82**, 840–844.
[29] K. Tanaka, N. Tatehata, K. Fujita and K. Hirao, *J. Appl. Phys.* 2001, **89**, 2213–2219.
[30] M. D. Regulacio, K. Bussmann, B. Lewis and S. L. Stoll, *J. Am. Chem. Soc.* 2006, **128**, 11173–11179.
[31] Y. Hasegawa, M. Kumagai, A. Kawashima, T. Nakanishi, K. Fujita, K. Tanaka and K. Fushimi, *J. Phys. Chem. C*. 2012, **116**, 19590–19596.

[32] Y. Hasegawa, M. Afzaal, P. O'Brien, Y. Wada and S. Yanagida, *Chem. Commun.* 2005, **2**, 242–243.
[33] W. L. Boncher, E. A. Görlich, K. Tomala, J. L. Bitter and S. L. Stoll, *Chem. Mater.* 2012, **24**, 4390–4396.
[34] Y. Ding, J. Gu, T. Zhang, A. X. Yin, L. Yang, Y. W. Zhang and C. H. Yan, *J. Am. Chem. Soc.* 2012, **134**, 3255–3264.
[35] S. Kar, W. L. Boncher, D. Olszewski, N. Dollahon, R. Ash and S. L. Stoll, *J. Am. Chem. Soc.* 2010, **132**, 13960–13962.
[36] R. S. Selinsky, J. H. Han, E. A. Morales Pérez, I. A. Guzei and S. Jin, *J. Am. Chem. Soc.* 2010, **132**, 15997–16005.
[37] T. Mirkovic, D. Rossouw, G. A. Botton and G. D. Scholes, *Chem. Mater.* 2011, **23**, 181–187.
[38] H. Masunaga, H. Ogawa, T. Nakashima, T. Kawai, T. Hikima, M. Takataa and S. Sasaki, *Dalton Trans.* 2013, **42**, 16216–16221.
[39] Y. P. Du, Z. Y. Yin, J. X. Zhu, X. Huang, X. J. Wu, Z. Y. Zeng, Q. Y. Yan and H. Zhang, *Nat. Commun.* 2012, **3**, 1177.
[40] Y. P. Du, B. Xu, T. Fu, M. Cai, F. Li, Y. Zhang and Q. B. Wang, *J. Am. Chem. Soc.* 2010, **132**, 1470–1471.
[41] Y. P. Du, Y. W. Zhang, Z. G. Yan, L. D. Sun and C. H. Yan, *J. Am. Chem. Soc.* 2009, **131**, 16364–16365.
[42] Y. P. Du, Y. W. Zhang, L. D. Sun and C. H. Yan, *J. Am. Chem. Soc.* 2009, **131**, 3162–3163.
[43] Y. P. Du, Y. Z. Yin, X. H. Rui, Z. Y. Zeng, X. J. Wu, J. Q. Liu, Y. Y. Zhu, J. X. Zhu, X. Huang, Q. Y. Yan and H. Zhang, *Nanoscale* 2013, **5**, 1456–1459.
[44] F. Zhao, H. L. Sun, S. Gao and G. Su, *J. Mater. Chem.* 2005, **15**, 4209–4214.
[45] Y. P. Du, Y. W. Zhang, Z. G. Yan, L. D. Sun, S. Gao and C. H. Yan, *Chem. Asian J.* 2007, **2**, 965–974.
[46] C. C. Kang, C. W. Lai, H. C. Peng, J. J. Shyue and P. T. Chou, *ACS Nano*. 2008, **2**, 750–756.
[47] Y. Hasegawa, Y. Okada, T. Kataoka, T. Sakata, H. Mori and Y. Wada, *J. Phys. Chem. B.* 2006, **110**, 9008–9011.
[48] C. X. Wang, D. Zhang, L. Xu, Y. N. Jiang, F. X. Dong, B. Yang, K. Yu and Q. Lin, *Angew. Chem. Int. Ed.* 2011, **50**, 7587–7591.
[49] F. Zhao, H. L. Sun, G. Su and S. Gao, *Small* 2006, **2**, 244–248.

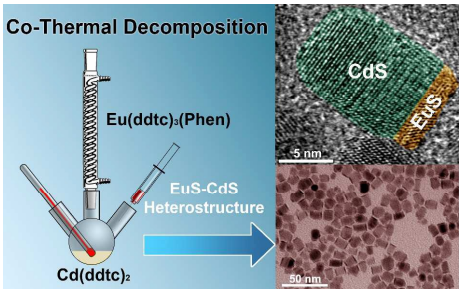

The EuS-CdS heterostructured nanocrystals which hold the unique optical-magnetic properties were synthesized from co-thermal decomposition method.